Superlattice Formation in a Binary Mixture of Block Copolymer Micelles

Sayeed Abbas and Timothy P. Lodge

Departments of Chemistry and Chemical Engineering & Materials Science, University of Minnesota, Minneapolis, Minnesota 55455, USA

(Received 25 April 2006; published 30 August 2006)

A binary solution mixture of distinct block copolymer micelles is found to adopt a superlattice. The larger micelles, formed from polystyrene-polyisoprene diblocks, have a nominal radius of 29 nm; the smaller micelles, formed from polystyrene-polydimethylsiloxane diblocks, have a nominal radius of 16 nm. The superlattice unit cell dimension is 156 nm and is assigned to space group $Fm\bar{3}c$; it corresponds to the AB_{13} structure. As these diblocks are uncharged, the driving force for superlattice formation is primarily free volume entropy, as in sterically stabilized colloidal hard spheres.

DOI: 10.1103/PhysRevLett.97.097803 PACS numbers: 61.25.Hq, 61.50.−f, 82.35.Jk, 83.80.Qr

Block copolymer solutions often exhibit two hierarchical levels of self-assembly, as the polymers first aggregate into discrete micelles and then the micelles pack on a lattice. For an AB diblock copolymer in a solvent that is selective for A, and where the micelles are approximately spherical, the known lattices are fcc, hcp, and bcc [1–4], although the $A15$ phase has also been considered [5,6]. Hexagonal, bicontinuous cubic, and lamellar phases are also common, for systems in which the unsolvated B domains occupy progressively larger volume fractions. Typically it requires 10–20 wt % copolymer or more to drive the micelles to adopt a lattice. Both thermotropic and lyotropic order-order transitions between these ordered phases have been studied in detail, as has the locus of order-disorder transitions between a lattice and a disordered solution of micelles or chains [1,2]. These various solvated lattices are interesting for diverse reasons, including their tunable mechanical and adhesive properties, as sieving media for DNA separations [7], as templates for growth of mesoporous inorganic materials [8], and for the controlled spatial distribution of functional nanoparticles [9,10]. Nevertheless, the possibility of introducing a third level of self-assembly, that of a superlattice between mixtures of distinct micellar units, is very appealing. Not only could new symmetries become accessible, but also the characteristic structural dimensions could be extended beyond the 10—100 nm range typically accessed. As far as we are aware, there have been no documented reports of superlattice formation in a mixture of block copolymer micelles.

The formation of superlattices [11] in sterically stabilized colloidal hard spheres has been carefully studied since the first observation of such a structure in certain natural opals [12–14]. The critical parameters are α, the ratio of the radii of the smaller (B) to the larger sphere (A), ρ, the ratio of the respective numbers of micelles, and ϕ, the overall volume fraction. Superlattices that have been documented include AB_2 (hexagonal, isomorphic to the compound AlB_2) [15,16], AB_6 (both simple cubic, isomorphic to CaB_6, and bcc, isomorphic to $C_{60}K_6$), [17] AB_{13} (simple cubic, isomorphic to $NaZn_{13}$) [15,16], and AB (bcc, isomorphic to CsCl) [18]. In general, the superlattice has been found to be in coexistence with other phases, either ordered or disordered, as either the composition ρ or the concentration ϕ is varied. The driving force for superlattice formation is free volume entropy, i.e., the overall packing fraction can be as great or greater than close-packed lattices of the separate spheres, and calculations of phase diagrams based on this supposition are in encouraging agreement with experiment [19]. The additional possibility that density differences can play a role has been called into question by the observation of superlattices for colloidal mixtures in zero gravity [17].

Inspired by this success with colloids, we have investigated whether a mixture of two block copolymer micelles could similarly adopt a superlattice. Block copolymer micelles are never strictly hard spheres, but for sufficiently large aggregation numbers and short corona blocks they are well known to adopt close-packed structures (fcc and hcp). An arbitrary combination of block copolymer micelles could exhibit a variety of transitions upon mixing, including macroscopic phase separation and intermicellar exchange of chains to form a single population of compositionally mixed micelles. In order to minimize any possible enthalpic interaction between micelles, we chose the corona blocks to be the same polymer, namely, polystyrene (S). In order to suppress chain exchange between two different micelles, we selected two different core blocks, polyisoprene (I) and polydimethyl siloxane (D), which do not mix at the chosen molecular weights. Furthermore, the solvent diethyl phthalate is strongly S selective, and the individual SI and SD micelles do not exhibit a critical micelle temperature (CMT) below 100 °C.

The particular SI(12-33) and SD(19-6) diblock copolymers were synthesized by standard anionic polymerization procedures [1]. The resulting block molecular weights, $M_S \approx 12\,000$ and $M_I \approx 33\,000$ g/mol for SI(12-33) and $M_S \approx 19\,000$ and $M_D \approx 33\,000$ g/mol for SD(19-6), were determined by a combination of size-exclusion chromatography and ^{1}H NMR spectroscopy. The polydispersity

indices were 1.01 and 1.06 for SI and SD, respectively. Diethyl phthalate (DEP) was obtained from Aldrich and purified according to standard procedures. A concentrated solution containing 16 vol % SD(19-6), 4% SI(12-33), and 80% DEP was prepared gravimetrically, using dioxane as a cosolvent. The dioxane was subsequently removed under vacuum. As dioxane is also selective for S, the two micelle populations were first created and mixed in the disordered state, and then compressed onto a lattice as the cosolvent was removed. The micelles were also characterized separately in dilute DEP solutions by dynamic light scattering. Mean hydrodynamic radii of 34 and 21 nm were obtained for SI(12-33) and SD(19-6), respectively, suggesting that for this system $\alpha \approx 0.6$. This value is close to those for which hard sphere systems have been observed to form AB_2 and AB_{13} superlattices [15,16]. Cryogenic transmission electron microscopy (cryo-TEM) was used to image a dilute mixture of micelles (1 vol % of each diblock in DEP), following procedures documented elsewhere [20]. A typical micrograph is shown in Fig. 1. Only the micellar cores are visible; the larger I cores are lighter, and the smaller D cores darker, due to electron density differences relative to the solvent. Measurements of the core radii (averaged over 30 micelles) gave mean core radii of 18 nm for SI(12-33) and 5 nm for SD(19-6). These values, coupled with the reasonable assumption of bulk polymer density within the cores, allow an estimate of the mean aggregation numbers: 400 for SI(12-33) and 50 for SD(19-6). From this we can estimate that there are about 60 SD micelles for each SI micelle in the concentrated mixture.

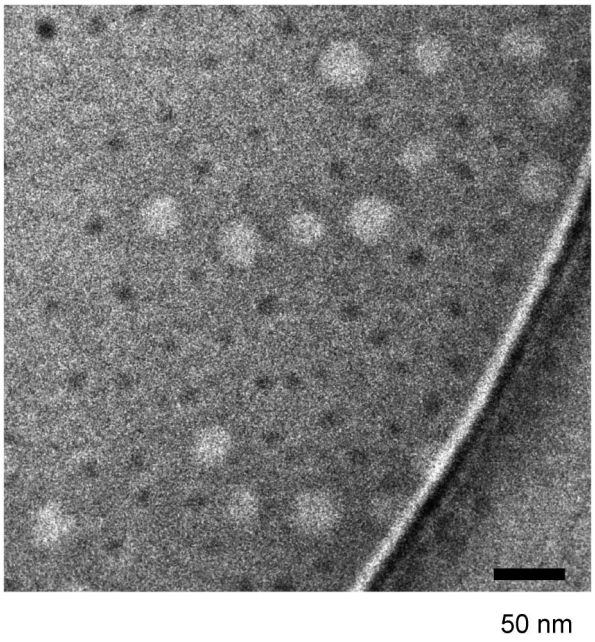

FIG. 1. Cryo-TEM image for 1 vol % of each diblock in DEP. The larger and lighter spheres belong to the isoprene core of the SI micelles, whereas the smaller and darker spheres belong to dimethylsiloxane core of the SD micelles.

Small angle x-ray scattering measurements were performed at the Advanced Photon Source, using a wavelength of 0.154 nm. The phase behavior of SI(12-33) in DEP has already been studied [1]. A 20% solution of SI(12-33) in DEP is disordered in room temperature, but on heating the micelles pack onto a close-packed fcc lattice with a lattice constant of 82 nm. On the other hand, a 20% solution of SD(19-6) in DEP packs onto an fcc lattice at room temperature with a lattice constant of 51 nm. These unit cell dimensions imply maximum equivalent hard sphere radii of 29 and 18 nm for SI(12-33) and SD(19-6), respectively. These values are systematically about 15% smaller than the dilute solution hydrodynamic radii, due to some corona compression in the ordered state, and possibly slightly smaller aggregation numbers. For the former copolymer, the fcc lattice is expected due to the relatively short corona block and large aggregation number; for the latter, one might have anticipated a bcc lattice. However, the CMT for 1% SI(12-33) in DEP is 150 °C, whereas the CMT of 1% SD(19-6) in DEP is higher than 200 °C, thus indicating that the interfacial tension between D and S + DEP is significantly greater. The stronger interfacial tension leads to a relatively high aggregation number for SD (19-6) micelles (given the short core block) and hence the fcc lattice is observed. A precedent for the phenomenon whereby stronger interfacial tension drives micelles to pack onto the fcc lattice exists: an SI(15-13) diblock packs onto a bcc lattice in dibutyl phthalate, whereas when the same diblock is dissolved in DEP (more strongly selective for S, hence higher interfacial tension) the fcc lattice is observed [1].

The azimuthally averaged small-angle x-ray scattering (SAXS) intensity for the 16% SI(12-33)/4% SD(19-6) mixed micelle solution is plotted as a function of wave vector in Fig. 2. The SAXS patterns were collected after the samples were stirred for 1 month. There are two clear sets of Bragg reflections in the figure. Those at lower q are indexed to a simple cubic structure ($q/q^* = 1, \sqrt{2}, \sqrt{3}, \sqrt{4}, \sqrt{5}, \sqrt{6}, \ldots$) and provide direct proof of the presence of a superlattice. The position of the first order reflection at $q^* = 0.0081$ Å^{-1} corresponds to a length scale substantially greater than observed in either micelle fcc lattice alone ($q^* \approx 0.0132$ and 0.021 Å^{-1} for SI and SD, respectively). The second, less well-resolved set of reflections at higher q (shown as an inset of Fig. 2) are due primarily to the coexistence of an fcc phase ($q/q^* = \sqrt{3}, \sqrt{4}, \sqrt{8}, \sqrt{11}, \sqrt{12}, \ldots$) of SI(19-6) micelles, with a slightly reduced, effective hard sphere radius of 16.4 nm. The coexistence of the SD(19-6) fcc phase is to be expected, given the large numerical excess of SD micelles in the mixture. The smearing of the fcc peaks in the mixture could be due to smaller fcc grain sizes caused by the coexisting phases. However, it is also likely that overlapping higher order peaks from the AB_{13} superlattice [such as the prominent (531) reflection [15]] are present.

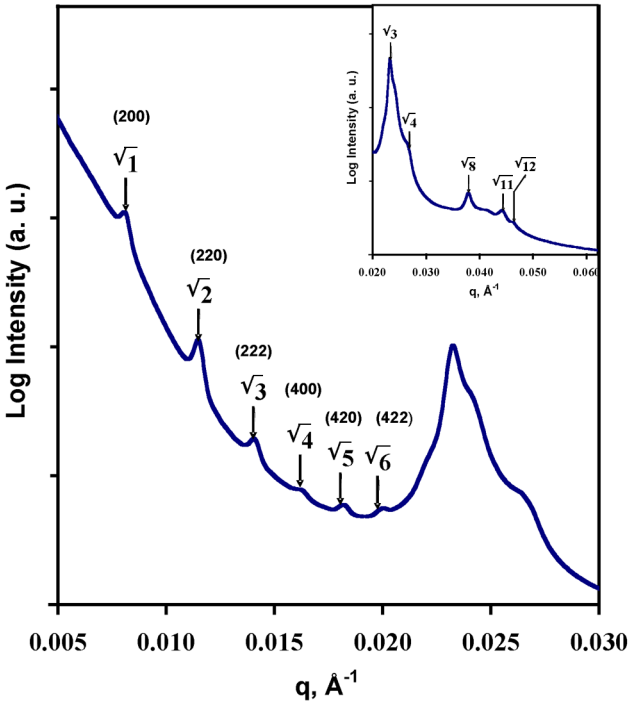

FIG. 2 (color online). One-dimensional SAXS pattern from the sample containing 16% SD(19-6), 4% SI(12-33) in 80% DEP. The peak ratios indicate a simple cubic lattice. Inset shows scattering pattern of the coexisting fcc phase. The peak ratios indicate an fcc lattice.

We now consider which superlattice is formed; two simple cubic precedents to consider are AB_{13} and AB_6. From Fig. 2 we observe unambiguous superlattice reflections only up to $\sqrt{6}$. Higher order peaks may be convoluted with the coexisting fcc peaks. Hence from these data we cannot confirm the existence or absence of a $\sqrt{7}$ peak, and therefore we should consider bcc AB_6 and AB lattices too. Overall, the evidence weighs heavily in favor of AB_{13}. This unit cell contains 112 spheres, 104 smaller and 8 larger micelles. The structure is more easily considered in terms of a subunit in which the larger spheres occupy the corners of a cube, and 12 smaller spheres are arranged inside on vertices of a virtual icosahedron, surrounding and touching a central small sphere; the subunit structure is shown in two projections in Fig. 3. Eight of these subunits form the unit cell, with the orientation of the icosahedra rotated by 90° between adjacent subcells. The primary peak in the scattering pattern from the AB_{13} lattice belongs to the (200) plane; hence the observed lattice constant ($d_{(100)}$) for the crystal is 156 nm. The packing fraction of the crystal (ϕ_{crys}) is estimated to be 72% (by taking the radius of the SD and SI micelles to be 16.4 and 29 nm, respectively). However, it should be noted here that ϕ_{crys} is very sensitive to the exact radius of the individual micelles. Since the micelles are actually not completely hard spheres and it is not required for the micelles to touch, it is difficult to estimate the radius precisely, and hence the value of ϕ_{crys} we report here has some uncertainty. Nevertheless, the estimate is appealingly close to the occupancy of a single close-packed lattice, supporting the interpretation of free volume entropy as the driving force for superlattice formation. Experimentally, the AB_{13} lattice has been observed with size ratios of $0.485 < \alpha < 0.62$ for hard spheres [15,21,22]. Monte Carlo simulations [19,23] predict the stability of AB_{13} lattice within the size range of $0.525 < \alpha < 0.62$, and cell model calculations [24] predict the stability range between $0.54 < \alpha < 0.62$. Thus, for the size ratio examined here, both theory and experiment provide a consistent explanation for the occurrence of the AB_{13} lattice.

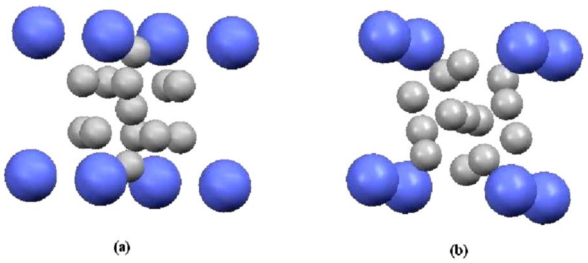

FIG. 3 (color online). Side view (a) and top view (b) of the AB_{13} subcell. The subcell consists of large spheres arranged on the vertices of a simple cube. A small sphere is located in the body-centered position surrounded by 12 other similar small spheres located on the vertices of an icosahedron. The entire unit cell consist of 8 such subcells with the orientation of the icosahedra rotated by 90° in subsequent subcells.

The simple cubic AB_6 lattice consists of bigger spheres occupying the vertices of a simple cube while the smaller spheres occupy the vertices of an octahedron inside the cube. For $\alpha = 0.62$, the hard spheres cubic AB_6 crystal has a packing fraction of approximately 0.38. The smaller spheres on the vertices of the octahedron touch each other. However, the bigger spheres do not touch any other sphere, thereby explaining the low packing fraction of the lattice. We conclude that the packing fraction of this lattice is too low to be consistent with the data.

The bcc AB_6 unit cell consists of bigger spheres occupying all the positions of a body-centered lattice, with the smaller spheres forming a square in each face of the larger cube. For $\alpha = 0.62$, the bcc AB_6 has a packing fraction of 0.48 for hard spheres. The smaller spheres touch each other, but the bigger spheres do not touch any other sphere. The low packing fraction of bcc AB_6 also makes the occurrence of this structure unlikely at $\alpha = 0.62$. Another bcc structure is the CsCl lattice. Here the bigger spheres occupy the vertices of a simple cube, whereas a smaller sphere occupies the body-centered position. For $\alpha = 0.62$, the packing fraction of this lattice is 0.64 and the bigger spheres touch each other along the (100) plane. The sphere at the body-centered position does not touch any other sphere. Density functional theories have rationalized the existence of the CsCl structure between 0.3 and 0.865

[25], and found it to be metastable in between 0.86 and 0.63 [26]; in contrast simulations [19] and cell model calculations [24] did not find this structure to be stable. From experiments, Schofield reported this structure at $\alpha = 0.736$ [18]; however, there were signs that the lattice was metastable. The theoretical $d_{(100)}$ spacing of the lattice formed by the SI and SD micelles is 58 nm, which is much lower than the observed spacing. We therefore conclude that our superlattice is not AB.

Based on the arguments given above, we conclude that AB_{13} is the most plausible structure. This conclusion is further supported by the fact that the relative heights of the superlattice peaks resemble very much those seen in colloids [22]. As mentioned before, the overall number ratio between the smaller (SD) and larger (SI) micelles is approximately 60:1. The SD micelles not taking part in the formation of the superlattice form the fcc lattice. It should be noted that the overlap of the fcc peaks with the presumed (531) reflection means that various other, related structures cannot be definitively ruled out; for example, the smaller sphere icosahedra may be randomly oriented. However, based on the strong experimental and theoretical precedents from colloidal spheres, the AB_{13} phase is by far the most probable.

In this Letter we report the first observation of a superlattice in a binary mixture of block SI and SD copolymer micelles. The lattice is assigned as AB_{13} and is found in coexistence with an fcc phase of the smaller SD micelles. The driving force is assumed to be free volume entropy, consistent with estimates of the packing fraction and with prior reports on colloidal hard spheres. There have recently been reports of an appealingly rich variety of superlattices in semiconductor and metallic nanoparticles [27,28] and charged colloids [29], but in these systems the free energy is dominated by electrostatics. Our results open the door to using block copolymers to generate new symmetries, and larger lattice constants, than can be obtained with single micelle systems.

This work was supported primarily by the MRSEC Program of the National Science Foundation under Grant No DMR-0212302. Use of the Advanced Photon Source was supported by the U.S. Department of Energy, Basic Energy Sciences, Office 8 of Science, under Contract No. W-31-109-Eng-38. Experiments were conducted at DND-CAT, which is supported by DuPont, Dow, NSF (No. DMR-9304725) and the Illinois Department of Commerce and Grant No. IBHE HECA NWU 96.

[1] T. P. Lodge, B. Pudil, and K. J. Hanley, Macromolecules **35**, 4707 (2002).
[2] K. J. Hanley, T. P. Lodge, and C. I. Huang, Macromolecules **33**, 5918 (2000).
[3] J. Bang *et al.*, Phys. Rev. Lett. **89**, 215505 (2002).
[4] G. A. McConnell *et al.*, Phys. Rev. Lett. **71**, 2102 (1993).
[5] M. Imai, I. Yoshida, T. Iwaki, and K. Nakaya., J. Chem. Phys. **122**, 044906 (2005).
[6] P. Ziherl and R. D. Kamien, Phys. Rev. Lett. **85**, 3528 (2000).
[7] B. Chu and D. Liang, J. Chromatogr. A **966**, 1 (2002).
[8] D. Zhao *et al.*, Science **279**, 548 (1998).
[9] Y. Lin *et al.*, Nature (London) **434**, 55 (2005).
[10] D. C. Pozzo and L. M. Walker, Macromol. Symp. **227**, 203 (2005).
[11] There is some variance in the literature in the use of the term superlattice. Strictly, the AB_{13} lattice can be called a superlattice as it is composed of distinct sublattices (8 in this case), whereas other binary lattices such as AB_2 and AB_6 should not. However, in the recent literature all of these (and more) have been referred to as superlattices. Hence in this Letter we conform to the less restrictive definition, but given that we interpret our structure as AB_{13}, the primary conclusion is unaffected.
[12] J. V. Sanders and M. J. Murray, Nature (London) **275**, 201 (1978).
[13] J. V. Sanders, Philos. Mag. A **42**, 705 (1980).
[14] M. J. Murray and J. V. Sanders, Philos. Mag. A **42**, 721 (1980).
[15] P. Bartlett, R. H. Ottewill, and P. N. Pusey, Phys. Rev. Lett. **68**, 3801 (1992).
[16] N. Hunt, R. Jardine, and P. Bartlett, Phys. Rev. E **62**, 900 (2000).
[17] D. Weitz *et al.*, NASA Report No. NASA/TM 2002-212011.
[18] A. B. Schofield, Phys. Rev. E **64**, 051403 (2001).
[19] M. D. Eldridge *et al.*, Mol. Phys. **84**, 395 (1995).
[20] J. Bang *et al.*, Macromolecules **39**, 1199 (2006).
[21] P. Bartlett, R. H. Ottewill, and P. N. Pusey, J. Chem. Phys. **93**, 1299 (1990).
[22] A. B. Schofield, P. N. Pusey, and P. Radcliffe, Phys. Rev. E **72**, 031407 (2005).
[23] M. D. Eldridge, P. A. Madden, and D. Frenkel, Mol. Phys. **79**, 105 (1993).
[24] X. Cottin and P. A. Monson, J. Chem. Phys. **102**, 3354 (1995).
[25] S. J. Smithline and A. D. J. Haymet, J. Chem. Phys. **86**, 6486 (1987).
[26] A. R. Denton and N. W. Ashcroft, Phys. Rev. A **42**, 7312 (1990).
[27] E. V. Shevchenko *et al.*, Nature (London) **439**, 55 (2006).
[28] F. X. Redl *et al.*, Nature (London) **423**, 968 (2003).
[29] A. P. Hynninen *et al.*, Phys. Rev. Lett. **96**, 138308 (2006).